LINEAR TRANSIENT FLOW SOLUTION FOR PRIMARY OIL RECOVERY WITH INFILL AND CONVERSION TO WATER INJECTION

Eric Zwahlen and Tad W. Patzek
U.C. Oil Consortium
Department of Materials Science and Mineral Engineering
591 Evans Hall, University of California at Berkeley
Berkeley, CA 94720

ABSTRACT

In this paper, we analyze the effects of primary production, producer infills and repressurization by water injection in a low-permeability, compressible, layered reservoir filled with oil, water and gas. The sample calculations are for the California Diatomites, but the equations apply to other tight rock systems. Primary oil recovery from rows of hydrofractured wells is described by linear transient flow of oil, water and gas with the concomitant pressure decline. During primary, it may be desirable to drill infill wells to accelerate oil production. At some later time, the infill wells may be converted into waterflood injectors for pressure support and incremental oil recovery. We analyze the pressure response and fluid flow rates for the original wells and infill wells drilled halfway between the original wells, and - finally - from water injection at the infill wells. All of the formation and fluid properties are described by a single hydraulic diffusivity assumed to be independent of time and production or injection. We solve the one-dimensional pressure diffusion equation analytically using pressure boundary conditions at the original and infill wells and use superposition to account for the water injection. We give solutions for the pressure in the formation, oil, water and gas rates and cumulatives at both the original wells and infill wells as functions of time. Finally, we present a computational example of oil production from a stack of seven independent diatomite layers with different properties and show the effects of infill wells and water injection on the total oil production. We show that a single-layer analytical solution and a 1-D numerical simulation for primary production in the diatomite agree well. Our analysis can predict the onset of pressure depletion and quantify how long to produce from the infill wells before injecting water. We show that producing from the infill well for a few years significantly increases the production from the field and can minimize the lost production at the infill well because of conversion to a waterflood injector.

INTRODUCTION

The late and middle Miocene diatomaceous oil fields in the San Joaquin Valley, California, are located in Kern County, some 40 miles west of Bakersfield. The largest oil volumes are found in the South, Middle and North Belridge Diatomite and Brown Shale, Lost Hills Diatomite and Brown Shale, Antelope Hills, McDonald Anticline, Chico-Martinez Chert, Cymric Diatomite, McKittrick, Railroad Gap, Belgian Anticline, Asphalto, Elk Hills, Buena Vista Antelope Shale, and Midway Sunset Reef Ridge and Antelope Shale. An estimated original oil in place (OOIP) in the Monterey diatomaceous fields exceeds 10 billion barrels and is comparable to that in Prudoe Bay in Alaska.

Cyclic bedding of the diatomite[1] is a well-documented phenomenon, attributed to alternating deposition of detritus beds, clay, and biogenic beds. The cycles span length scales that range from a fraction of an inch to tens of feet, reflecting the duration of depositional phases from semiannual to thousands of years. On a large scale, there are at least seven distinct oil producing layers with good lateral continuity within each layer, but little vertical continuity between adjacent layers. The diatomites are very porous (25 to 65 percent), rich in oil (35 to 70 percent), and nearly impermeable (0.1 to 10 millidarcies). The high porosity and oil saturation, together with large thickness (up to 1000 feet) and area (up to a few square miles per field) translate into the gigantic OOIP estimates.

To compensate for the low reservoir permeability, all wells in the diatomite must be hydrofractured. A typical well has 3 to 8 fractures with an average fracture half-length of 150 feet. Wells are usually spaced along lines following the maximum in-situ stress every 330 feet (2-1/2-acre), 165 feet (1-1/4-acre) or even 82 feet (5/8-acre). Thousands of hydrofractures have been already induced and thousands more may be created as new recovery processes, such as waterflood,[2-4] or steam drive [5,6] on 5/8 acre spacing, become commercially viable.

Primary oil production on 2-1/2-acre spacing, followed by infill to 1-1/4 acre and subsequent conversion to waterflood is of great interest to the producers of the diatomaceous oil fields. We start from the mathematical formulation of the problem. We then present a computational example of a seven-layer diatomite reservoir. We also compare a single-layer analytical solution for primary production with a 1-D reservoir simulation. In Appendix A, we list several correlations of PVT properties of oil and solution gas.

PROBLEM STATEMENT

In a compressible, homogeneous porous medium, the pressure distribution follows a simple diffusion equation. With suitable boundary conditions and an initial condition, the pressure and fluid velocity in the medium can be calculated analytically. In this paper, we analyze a reservoir at some uniform initial pressure p_i at $t = 0$. First, we drill a series of wells with spacing $2L$ and wellbore flowing pressure p_{well}. All wells are hydrofractured, and all of the fractures are rectangular and have permeabilities that are much higher than the formation permeability. Therefore, we can assume that the uniform pressure p_{well} is imposed throughout the entire hydrofracture. Second, at some time $t_{\inf}$, we drill infill wells halfway between the original wells and also produce these wells at p_{well}. Third, at time t_{inj}, we inject water into the infill wells at the downhole injection pressure p_{inj} and continue producing at the original wells. This final step is to quantify the effect of repressurization of the formation.

This statement of primary production, followed by infill and injection, is a simplification of what actually occurs. Here we assume uniform and constant properties in each layer and constant pressures in the wells, and we neglect the effect production and injection may have on fluid and rock properties. We assume each of the layers in the reservoir is independent, solve the problem for each layer separately, and add the individual layer solutions. These assumptions allow us to derive an analytical solution that can show us the effect of each of the system parameters on the production.

Original Primary Production

The one-dimensional pressure diffusion equation is

$$\frac{\partial p}{\partial t} = \alpha \frac{\partial^2 p}{\partial x^2}, \quad 0 \le x \le L, \qquad t > 0 \tag{1}$$

where

$$\alpha = \frac{\lambda_t}{\phi c_t} \tag{2}$$

is the hydraulic diffusivity, which accounts for the total compressibility of the formation, c_t, and the total fluid mobility, λ_t. All of the formation and fluid properties are combined into the single constant parameter α (see Appendix A). As mentioned, we assume α remains constant during production and injection.

From symmetry we write the equations only for $0 \le x \le L$, where the original wells are at $x = \pm L$. The initial condition is uniform pressure everywhere in the layer,

$$p(x,0) = p_i, \qquad 0 \le x \le L. \tag{3}$$

The boundary conditions for primary production are

$$\left.\begin{aligned} \frac{\partial p}{\partial x}(0,t) &= 0 \\ p(L,t) &= p_{well} \end{aligned}\right\}, \qquad t < t_{inf} \tag{4}$$

Before the infill time, the symmetry halfway between the original wells at $x = 0$ requires a no-flow boundary condition, which is specified by the gradient of the pressure being equal to zero. The pressure at the primary production well at $x = L$ is specified as the well flowing pressure.

This system of equations can be solved by separation of variables.[7] The zero-gradient condition at $x = 0$ leads to a cosine expansion of the initial condition. The pressure before infill is

$$p(x,t) = p_{well} + 2(p_i - p_{well})\sum_{n=0}^{\infty}(-1)^n \frac{\cos(\lambda_n x / L)}{\lambda_n} e^{-\lambda_n^2 \alpha t / L^2}, \quad 0 \le x \le L, \quad 0 < t < t_{inf} \tag{5}$$

where

$$\lambda_n = (2n+1)\frac{\pi}{2}, \qquad n = 0,\ 1,\ 2,\ \ldots \tag{6}$$

This cosine series clearly shows that the boundary conditions before the infill time are satisfied. The time dependence of the pressure is controlled by α divided by L^2.

An alternate form of the solution, obtained most easily by Laplace Transform, is better suited for early times[7]:

$$p(x,t) = p_{well} + (p_i - p_{well})\left[1 - \sum_{n=0}^{\infty}(-1)^n \left\{\operatorname{erfc}\frac{(2n+1) - x/L}{2\sqrt{\alpha t / L^2}} + \operatorname{erfc}\frac{(2n+1) + x/L}{2\sqrt{\alpha t / L^2}}\right\}\right] \tag{7}$$

$$0 \le x \le L,\ t > t_{inf}$$

We can obtain the average pressure $\bar{p}$ in the reservoir by integrating the pressure profile from $x = 0$ to $x = L$ and then dividing by L:

$$\bar{p}(t) = \frac{1}{L}\int_0^L p(x',t)\ dx' \tag{8}$$

Alternatively we can consider a “pressure” balance on the system. This is actually an energy balance where the energy density is p / L. Then the average pressure is the initial uniform pressure minus the “lost” pressure that has flowed out the boundary:

$$\bar{p}(t) = p_i - \frac{1}{L}\int_0^t \left(-\alpha \left.\frac{\partial p}{\partial x}\right|_{x=L} \right) dt' \tag{9}$$

Inserting the pressure distribution given in (5) into (8) gives the average pressure on primary as

$$\bar{p} = p_{well} + 2\left(p_i - p_{well}\right)\sum_{n=0}^{\infty}\frac{e^{-\lambda_n^2 \alpha t / L^2}}{\lambda_n^2} \tag{10}$$

The average pressure from the complimentary error function solution is most easily obtained using (9). Then the average pressure is

$$\bar{p} = p_i - 2\left(p_i - p_{well}\right)\sqrt{\alpha t / L^2}\left\{\frac{1}{\sqrt{\pi}} + 2\sum_{n=1}^{\infty}(-1)^n \operatorname{ierfc}\left(\frac{n}{\sqrt{\alpha t / L^2}}\right)\right\} \tag{11}$$

where

$$\operatorname{ierfc}(z) = \frac{1}{\sqrt{\pi}}e^{-z^2} - z\operatorname{erfc}(z) \tag{12}$$

The ierfc function is negligible for large arguments (early times), so this equation clearly shows that the average pressure initially drops linearly with the square root of time.

Primary After Infill

At the infill time, an infill well is drilled at $x = 0$, and the pressure is specified at both boundaries of the system. This set of boundary conditions leads to a sine series expansion of the original cosine series. We set $t = t_{\text{inf}}$ in (5) and use the result as the initial condition for a new set of side conditions to solve (1). The initial condition is

$$p\left(x, t_{inf}\right) = p_{well} + 2\left(p_i - p_{well}\right)\sum_{n=0}^{\infty}(-1)^n \frac{\cos\left(\lambda_n x / L\right)}{\lambda_n} e^{-\lambda_n^2 \alpha t_{inf} / L^2}, \quad 0 \le x \le L \tag{13}$$

The boundary conditions are specified as constant-pressure conditions by

$$\left.\begin{aligned} p(0,t) &= p_{well} \\ p(L,t) &= p_{well} \end{aligned}\right\}, \qquad t \ge t_{inf} \tag{14}$$

Again by separation of variables, the solution to (1) is given by

$$p(x,t) = p_{well} + 4(p_i - p_{well})\sum_{m=1}^{\infty} \beta_m \sin\left(\frac{\beta_m x}{L}\right) e^{-\beta_m^2 \alpha (t - t_{inf})/L^2} \sum_{n=0}^{\infty} \frac{(-1)^n e^{-\lambda_n^2 \alpha t_{inf}/L^2}}{\lambda_n \left(\beta_m^2 - \lambda_n^2\right)}, \tag{15}$$

$0 \le x \le L,\ t > t_{inf}$

where

$$\beta_m = m\pi, \qquad m = 1,\ 2,\ 3,\ \ldots \tag{16}$$

<ins>Oil Flow Rate Before Infill</ins>

The oil flow rate is proportional to the derivative of the pressure in the reservoir. The oil flow rate at the original primary wells is

$$q_o^{(1)} = -A \frac{kk_{ro}}{\mu_o} \left.\frac{\partial p}{\partial x}\right|_{x=L} \tag{17}$$

where A is twice the area of the production well hydrofractures, with the factor of 2 coming from symmetry (there are actually two production wells or, alternatively, two sides of a hydrofracture). The superscript (1) refers to the original wells. Differentiating the pressure solution in (5) and using the definition of the flow rate gives the flow rate before infill:

$$q_o^{(1)} = 2A \frac{kk_{ro}}{\mu_o} \frac{\left(p_i - p_{well}\right)}{L} \sum_{n=0}^{\infty} e^{-\lambda_n^2 \alpha t/L^2}, \quad 0 \le t \le t_{inf} \tag{18}$$

An alternate form that explicitly shows the early inverse square-root-of-time behavior is obtained by differentiating (7) as

$$q_o^{(1)} = A \frac{kk_{ro}}{\mu_o} \frac{\left(p_i - p_{well}\right)}{\sqrt{\pi \alpha t}} \left\{ 1 + 2\sum_{n=1}^{\infty} (-1)^n e^{-\left(\frac{n}{\sqrt{\alpha t/L^2}}\right)^2} \right\},\ 0 \le x \le L,\ t < t_{inf} \tag{19}$$

At early times the exponential function is approximately zero, so the effect of the summation is negligible. By substituting for α in (19) we can see that the oil flow rate is proportional to $\sqrt{\dfrac{kk_{ro}\phi c_t}{\mu_o}}$.

Oil Flow Rate After Infill

After the infill well is drilled, oil is produced from both the original well and the new infill well. After infill, the oil flow rate can be obtained by differentiating (15). The oil flow rate at the original wells is

$$q_o^{(1)} = -4A\frac{kk_{ro}}{\mu_o}\frac{\left(p_i - p_{well}\right)}{L}\sum_{m=1}^{\infty}(-1)^m\beta_m^2 e^{-\beta_m^2\alpha\left(t-t_{inf}\right)/L^2}\sum_{n=0}^{\infty}\frac{(-1)^n e^{-\lambda_n^2\alpha t_{inf}/L^2}}{\lambda_n\left(\beta_m^2-\lambda_n^2\right)},\ \ t \ge t_{inf} \tag{20}$$

After infill, the oil flow rate at the infill well is

$$q_o^{(2)} = -4A\frac{kk_{ro}}{\mu_o}\frac{\left(p_i - p_{well}\right)}{L}\sum_{m=1}^{\infty}\beta_m^2 e^{-\beta_m^2\alpha\left(t-t_{inf}\right)/L^2}\sum_{n=0}^{\infty}\frac{(-1)^n e^{-\lambda_n^2\alpha t_{inf}/L^2}}{\lambda_n\left(\beta_m^2-\lambda_n^2\right)},\quad t \ge t_{inf} \tag{21}$$

where the superscript (2) refers to the infill well.

Cumulative Oil Production

We are also interested in the total volume of oil that is produced from the original wells and the infill wells. The cumulative oil production up to some time t is given by

$$Q_o = \int_0^t q_o\, dt' = -A\frac{kk_{ro}}{\mu_o}\int_0^t \frac{\partial p}{\partial x}\, dt' \tag{22}$$

Before infill, the cumulative production at the primary wells is

$$Q_o^{(1)} = 2A\frac{kk_{ro}}{\mu_o}\frac{\left(p_i - p_{well}\right)}{L}\frac{L^2}{\alpha}\sum_{n=0}^{\infty}\frac{\left(1-e^{-\lambda_n^2\alpha t/L^2}\right)}{\lambda_n^2},\quad 0 \le t \le t_{inf} \tag{23}$$

An alternative form that explicitly shows the square-root-of-time dependence is obtained from the complimentary error function solution as

$$Q_o^{(1)} = 2A\frac{kk_{ro}}{\mu_o}\frac{\left(p_i - p_{well}\right)}{\alpha}\sqrt{\alpha t}\left\{\frac{1}{\sqrt{\pi}} + 2\sum_{n=1}^{\infty}(-1)^n \operatorname{ierfc}\left(\frac{n}{\sqrt{\alpha t / L^2}}\right)\right\},\ 0 \le x \le L,\ t < t_{inf} \qquad (24)$$

The ierfc function for large arguments is approximately zero; hence the summation term is negligible for early times.

At the infill time, the cumulative production at the original well is

$$Q_{o,inf}^{(1)} = 2A\frac{kk_{ro}}{\mu_o}\frac{\left(p_i - p_{well}\right)}{L}\frac{L^2}{\alpha}\sum_{n=0}^{\infty}\frac{\left(1 - e^{-\lambda_n^2 \alpha t_{inf}/L^2}\right)}{\lambda_n^2} \qquad (25)$$

After infill, the cumulative production at the original well is

$$Q_o^{(1)} = Q_{o,inf}^{(1)} + \int_{t_{inf}}^{t} q_o^{(1)}\, dt' = Q_{o,inf}^{(1)} - A\frac{kk_{ro}}{\mu_o}\int_{t_{inf}}^{t}\left.\frac{\partial p}{\partial x}\right|_{x=L} dt' \qquad (26)$$

Thus from the original production wells

$$Q_o^{(1)} = Q_{o,inf}^{(1)} - 4A\frac{kk_{ro}}{\mu_o}\frac{\left(p_i - p_{well}\right)}{L}\frac{L^2}{\alpha}\sum_{m=1}^{\infty}(-1)^m\left(1 - e^{-\beta_m^2\alpha\left(t - t_{inf}\right)/L^2}\right)\sum_{n=0}^{\infty}\frac{(-1)^n e^{-\lambda_n^2 \alpha t_{inf}/L^2}}{\lambda_n\left(\beta_m^2 - \lambda_n^2\right)},\ t \ge t_{inf} \qquad (27)$$

At the infill well, the cumulative production is

$$Q_o^{(2)} = 4A\frac{kk_{ro}}{\mu_o}\frac{\left(p_i - p_{well}\right)}{L}\frac{L^2}{\alpha}\sum_{m=1}^{\infty}\left(1 - e^{-\beta_m^2\alpha\left(t - t_{inf}\right)/L^2}\right)\sum_{n=0}^{\infty}\frac{(-1)^n e^{-\lambda_n^2 \alpha t_{inf}/L^2}}{\lambda_n\left(\beta_m^2 - \lambda_n^2\right)},\ \ t \ge t_{inf} \qquad (28)$$

Water Injection at Infill Well

Finally, we investigate the effect of water injection at the infill well in order to repressurize the formation. This approach is admittedly approximate for water injection as it neglects the effect of incompressible Buckley-Leverett displacement of the oil by the injected water, as well as water imbibition. We assume the rock and fluid compressibilities continue to be the same as originally present in the formation. We then calculate the pressure in the system, the rate of injection and cumulative injection of water, and the rate and cumulative production of oil at the original well.

Because of the linearity of the equations, this water injection problem can be solved by superposition. We continue to calculate the pressure, flow rate, and cumulative production at the infill well using the equations previously discussed. The total pressure, injection, and production will be the sum of the previous infill problem and the following injection problem. The equations for the water injection calculation are

$$\frac{\partial p_{inj}}{\partial t} = \alpha \frac{\partial^2 p_{inj}}{\partial x^2}, \qquad 0 \le x \le L, \qquad t > t_{inj} \tag{29}$$

For simplicity, we use the same hydraulic diffusivity α in this injection problem as in the previous infill problem to describe the compressibility of the formation and the fluids. The initial condition is

$$p_{inj}(x, t_{inj}) = p_{well}, \qquad 0 \le x \le L \tag{30}$$

This states that the initial pressure for this injection superposition calculation is the well flowing pressure. The boundary conditions are

$$\left.\begin{aligned} p_{inj}(0,t) &= p_{inject} \\ p_{inj}(L,t) &= p_{well} \end{aligned}\right\}, \qquad t > t_{inj} \tag{31}$$

The pressure at the infill well (now an injector) is prescribed as p_{inject} and the pressure at the original production well is prescribed as p_{well}.

We define a normalized pressure that scales the injection pressure to the original formation pressure:

$$p^* = \frac{p_{inject} - p_{well}}{p_i - p_{well}} \tag{32}$$

The solution for the pressure in the formation only from water injection is

$$p_{inj}(x,t) = p_{well} + p^*(p_i - p_{well})\left\{1 - \frac{x}{L} - 2\sum_{m=1}^{\infty}\frac{\sin(\beta_m x/L)}{\beta_m}e^{-\beta_m^2\alpha(t-t_{inj})/L^2}\right\}, 0 \le x \le L, t > t_{inj} \quad (33)$$

The water injection rate at the infill well is

$$q_{w,inj}^{(2)} = A\frac{kk_{rw}}{\mu_w}\frac{(p_i - p_{well})}{L}p^*\left\{1 + 2\sum_{m=1}^{\infty}e^{-\beta_m^2\alpha(t-t_{inj})/L^2}\right\}, \quad t > t_{inj} \quad (34)$$

Here the subscript *w* refers to water and the subscript *inj* indicates injection.

The cumulative water injection at the infill well from water injection alone is

$$Q_{w,inj}^{(2)} = A\frac{kk_{rw}}{\mu_w}\frac{(p_i - p_{well})}{L}\frac{L^2}{\alpha}p^*\left\{(t - t_{inj}) + 2\sum_{m=1}^{\infty}\frac{\left(1 - e^{-\beta_m^2\alpha(t-t_{inj})/L^2}\right)}{\beta_m^2}\right\}, \quad t > t_{inj} \quad (35)$$

The oil production rate at the original well from only the water injection is

$$q_{o,inj}^{(1)} = A\frac{kk_{ro}}{\mu_o}\frac{(p_i - p_{well})}{L}p^*\left\{1 + 2\sum_{m=1}^{\infty}(-1)^m e^{-\beta_m^2\alpha(t-t_{inj})/L^2}\right\}, \quad t > t_{inj} \quad (36)$$

The cumulative oil production at the original well from the water injection is

$$Q_{o,inj}^{(1)} = A\frac{kk_{ro}}{\mu_o}\frac{(p_i - p_{well})}{L}\frac{L^2}{\alpha}p^*\left\{(t - t_{inj}) + 2\sum_{m=1}^{\infty}(-1)^m\frac{\left(1 - e^{-\beta_m^2\alpha(t-t_{inj})/L^2}\right)}{\beta_m^2}\right\}, \ t > t_{inj} \quad (37)$$

Total Pressure, Flow Rates, and Cumulative Production by Superposition

We now present the superposition equations necessary to calculate the net pressure, flow rates, and cumulative production after water injection begins. The linearity of the equations allows us to add the results of the infill problem to the results of the injection problem to get the total.

The total pressure in the formation is sum of the pressure calculated by the original solution for *p* and the solution for p_{inj}:

$$p^{net} = p + p_{inj} - p_{well}, \quad t > t_{inj} \quad (38)$$

After water injection begins at an infill well, there is no more oil production from this well. The net rate of water injection is given by the water injection rate from the injection problem minus the oil production rate calculated from the original infill problem,

$$q_{w,inj}^{(2),net} = q_{w,inj}^{(2)} - q_o^{(2)}, \qquad t > t_{inj} \tag{39}$$

We let $Q_{o,inj}^{(2)}$ be the cumulative oil production at the infill well up until the time at which water injection begins. Then the net cumulative water injection is given by

$$Q_w^{(2),net} = Q_{w,inj}^{(2)} - \left(Q_o^{(2)} - Q_{o,inj}^{(2)}\right), \qquad t > t_{inj} \tag{40}$$

The net oil production rate at the original well $q_o^{(1),net}$ is

$$q_o^{(1),net} = q_o^{(1)} + q_{o,inj}^{(1)}, \qquad t > t_{inj} \tag{41}$$

The net cumulative oil production at the original well is

$$Q_o^{(1),net} = Q_o^{(1)} + Q_{o,inj}^{(1)}, \qquad t > t_{inj} \tag{42}$$

COMPUTATIONAL EXAMPLE

As an example, we model a portion of Section 33 in the South Belridge diatomite field. This region can be divided into seven separate layers (diatomite cycles), each with its own material and fluid properties. For each layer, we assume that the initial producer spacing is 330 feet (2-1/2-acre), and the tip-to-tip length of the hydrofracture is also 330 feet. The properties of each layer are summarized in Table 1. These data are averages of well log data taken at one-foot intervals through the reservoir column.

The depth is to the middle of each layer where the temperature and pressure are calculated. We assume that the layer pressure corresponds to the oil bubblepoint pressure for a particular layer. The bubblepoint pressure as a function of depth is then given by

$$p_{bp} = 29.7 + 0.438 \times \text{depth(ft)}, \quad \text{psia} \tag{43}$$

The layer temperature is calculated from the average thermal gradient for the diatomite, which is given as

$$T = 72.0 + 0.024 \times \text{depth(ft)}, \quad {}^{\circ}\text{F} \tag{44}$$

Table 1. Diatomite Layer Properties

LAYER	THICK-NESS, ft	DEPTH, ft	ϕ	k, md	S_o	S_g	$S_o \times \phi$	Oil in Place, MSTBO
G	206	733	0.57	0.15	0.56	0.11	0.32	1275
H	120	896	0.57	0.15	0.38	0.14	0.22	504
I	160	1036	0.54	0.12	0.36	0.14	0.19	603
J	160	1196	0.56	0.14	0.43	0.13	0.24	747
K	42	1297	0.57	0.16	0.51	0.12	0.29	236
L	162	1399	0.54	0.24	0.40	0.13	0.21	678
M	140	1550	0.51	0.85	0.30	0.15	0.16	415

To get a quantitative estimate of the productivity of a layer, we must calculate its α from the parameters listed in Table 2. The relative permeabilities are calculated using the Stone II model discussed in Appendix A with the parameters given in Table 3. The large variation in k_{ro} leads to large variation in λ_t and α. The viscosity and total compressibility decrease monotonically from the top layer to the bottom layer.

Table 2. Calculated Diatomite Layer Properties

LAYER	k_{ro}	μ, cp	$c_t \times 10^6$, 1/psi	λ_t, md/cp	α, ft^2/D
G	0.45	6.1	1233	0.0636	0.573
H	0.076	5.5	875	0.0106	0.135
I	0.024	5.0	747	0.0027	0.042
J	0.21	4.6	705	0.0265	0.425
K	0.40	4.3	707	0.0584	0.919
L	0.096	4.1	584	0.0212	0.426
M	0.013	3.8	488	0.0102	0.260

Table 3. Parameters for Stone II Relative Permeability Model

Parameter	S_{wc}	S_{orw}	S_{org}	S_{gr}	k_{rocw}	k_{rwro}	k_{rgro}	n_w	n_{ow}	n_{og}	n_g
Value	0.4[a]	0.35[b]	0.25[c]	0.05	1.0	0.15	1.0	3.5	2.5	2.0	1.5

[a]0.3 in layer G, 0.35 in layer K
[b]0.3 in layer H, 0.3 in layer H, 0.2 in layer M
[c]0.2 in layer M

Layer K has the highest α and will react the fastest and produce well. However, it is a thin layer with little oil in place, so the total volume will be small. Layers G, J, L, and M have intermediate values of α and good amounts of oil, so they will be good producers. Layers H and I have the lowest values of α, will produce poorly and show little effect of infill and water injection.

We impose a backpressure of 50 psi on the producers. The original wells produce for 5 years (1825 days) or 10 years (3650 days), after which an infill well is drilled between them. After one year of production from the infill well, at 6 years (2190 days) or 11 years (4015 days), water is injected at p_{inject} into the infill well, where

$$p_{inject} = 0.7 \times \text{depth(ft)}, \quad \text{psia} \tag{45}$$

i.e., we assume maximum possible water injection pressure in each layer.

Table 4 lists the other parameters used, which are independent of other layer properties.

Table 4. Layer-Independent Parameters Used in the Calculations

Description	Value
Oil Gravity (°API)	29
Rock compressibility ($\text{psi}^{-1} \times 10^6$)	30
γ_g, gravity of separator gas	0.864
WOR (STB/STB)	0.6
GOR (mscf/STB)	0.6
Convergence criterion	1×10^{-8}

These parameter values are used to calculate the pressure, oil flow rate at the wells, and cumulative oil production from each layer as a function of time. The cumulative production and percent oil recovery are of most interest, and the results are shown in the following figures as a function of the square root of time, giving straight lines for early times. All calculations are carried out for 50 years (18,250 days = 135 day$^{1/2}$).

Figure 1 shows the cumulative production in thousands of barrels in each layer and the total for 50 years without infill or injection. The slope of the total primary production is approximately 3000 STBO/day$^{1/2}$, which is representative of a very good well in the diatomite. A poorer well might not have the entire hydrofracture area open, or it might have and the production would be less.

Layer G, which has the most oil in place and high α, produces the most oil. The next two layers, H and I, have low oil saturations and low α values and are poor producers. The deeper layers have high α values and are good producers. Layer K has a low cumulative production because it has little oil in place.

Figure 2 shows the percent oil recovery of all of the layers and the total for 50 years. The total is recovery is about 10 percent, with the deeper layers J through M better and the top layers G through I worse.

Figure 3 shows the percent oil recovery and water injection for infill at 5 years and water injection at 6 years. Figure 4 shows the same results for infill at 10 years and water injection at 11 years. These figures show the percent oil recovery and water injection for each layer in the formation calculated as the volume produced or injected divided by the original oil in place times 100. The final total increase in recovery from injection is about 3 percent. The scale of each figure, except layer K, is the same so that the layers can be easily compared.

Each of the plots has five separate curves. The top curve, shown as a bold solid line, is the percent oil recovery from the original well, including the effect of the infill well and water injection. The upward trend at late times is from the extra oil produced by water injection. The normal solid line is the percent oil recovery at the original well with infill but without injection at the infill well. In most of the layers, the difference between recovery with and without injection is about 3 percent. In layer K the effect is rapid and large, because of the high α. However, we stress that much of the increased recovery in this layer at late times may be just from the injected water recirculated through the producer. Layers H and I show almost no effect of the water injection because of low oil saturation and low α. This calculation shows that in the absence of Buckley-Leverett banking of oil, the incremental oil recovery from pressure support by water injection will be small. Hence, in layers with a low oil saturation or unfavorable mobility ratio, one cannot expect a big waterflood response.

The first dotted curves show the percent oil recovery at the infill well where production starts from zero at the infill time. The “Infill (no injection)” curves in Figures 3 and 4 show the production if there were no injection, and the “Infill (with injection)” curves show the production with injection. These latter recovery curves (including water injection) become flat after water injection begins because no more oil is produced at the infill well. For most of the layers, a significant amount of oil production from the infill well is lost because of injection. However, injection may be necessary to preserve the integrity of the formation and decrease well failure. Thus, producing from the infill well for two to five years before injection begins instead of just one may be better.

The water injection curve is the volume of water injected divided by the original oil in place in the layer times 100 to keep the units consistent. Even though the injection begins at about six years, the effect at the original wells is not seen until almost 20 years. Layer K shows the effect sooner, but layers H and I show almost no effect of injection even at 50 years. The rate of water injection becomes constant at late times. The percent recovery rises linearly with time for late times, but appears to bend upward when plotted here versus the square root of time.

To further explain the figures, we specifically consider layer G. We see from Figure 1 that the total volume of oil produced in 50 years is approximately 100 MSTBO with no infill or injection, which is about 8 percent recovery. With infill and injection the original well produces just under 9 percent or 110 MSTBO, and the infill well produced an additional 15 MSTBO in the one year of production. The 15 MSTBO could be increased to about 30 MSTBO if water injection began at eight years instead of six.

Figure 5 shows the pressure profiles for infill at 10 years and water injection at 11 years for layers G, I, K, and M. These layers show representative values of α with layer I having the lowest and layer K the largest value. Large values of α give a faster pressure response. In these figures, the position labeled 0 feet is the position of the infill well, and the position at 165 feet is the original well. The pressure at the original well is constant at 50 psia.

In Figure 5A, the initial pressure in layer G is 350 psia and the pressure at the "original" well is maintained at 50 psia. The pressure profile at $x = 0$ is horizontal until 10 years, indicating the no-flow (or symmetry) boundary condition. At 10 years when the infill well is drilled, the pressure at $x = 0$ has not decreased significantly. The 11th year profile is just before injection at 513 psia begins at the infill well. Finally, the pressure distribution becomes a linear, steady-state profile with injection.

Layer I, shown in Figure 5B, reacts much slower than the other layers. The initial pressure is 480 psia. By 10 years when the infill well is drilled, the pressure wave is only about a quarter of the way in from the original well. Even at 50 years, the steady state is not yet reached. The infill and injection does not significantly affect the original well.

Layer K, shown in Figure 5C, has the highest α, and the pressure wave reaches the infill well position at five years. By 10 years the pressure has dropped enough so that oil production at the original well is also falling. After injection begins, the steady state is nearly reached in 15 to 20 years.

Layer M, shown in Figure 5D, appears very similar to layer G. Even though layers G and M have different properties, their α values are similar, which results in similar pressure responses.

COMPARISON WITH NUMERICAL SIMULATOR

We now compare the results of a single-layer analytical solution with a 1-D compositional simulation, using an industry standard simulator THERM[11]. As total oil production is a summation over the independent reservoir layers, this comparison is all that is needed to validate our analytical model. The numerical simulation is of primary production on 2-½ acres. As shown in Figures 6 and 7, the two analyses give nearly the same results. The data for the simulation, shown in Table 5, are for a deep layer, e.g., layer M, but with a moderate permeability and high oil saturation. The depth in the analytical solution was chosen to match the initial pressure in the simulation. The well flowing pressure is fixed at 100 psia in both cases. The only parameters that are different in the two calculations are k_{ro} and μ, both of which are inputs in the analytical solution.

Table 5. Parameters for Comparison with THERM

	DEPTH, ft	THICK-NESS, ft	ϕ	k, md	kk_{ro}, md	μ, cp	°API	c_f	S_o	S_g	S_{orw}	S_{gc}
THERM	NA	150	0.58	0.17	0.07	5-6	28	25	0.56	0.085	0.25	0.05
Analytical Solution	1550	150	0.58	0.17	0.08	4.5	28	25	0.56	0.085	0.25	0.05

Figure 6 compares the percent oil recoveries. The THERM simulation is carried to 36 years and the analytical solution to 50 years. Until the very end of the numerical simulation, the results are similar. The simulation predicts a lower ultimate recovery, because depletion changes the properties of the system. Thus α is not actually constant for the entire production time because the volatile oil components are produced preferentially. However, the difference is not significant until after 30 years.

Figure 7 compares the average pressure in the layer. The analytical solution uses Eq. (10). The average pressure predicted by the analytical solution falls slightly slower than that predicted by THERM. Also near the end of the simulation, the pressure flattens out more quickly, and the production slows down. This is caused by the preferential depletion of solution gas in the simulation and gradual decrease of overall system compressibility.

Our simple analytical model can accurately predict the recovery and pressures for primary production. The PVT properties and relative permeabilities agree well with those predicted by THERM.

CONCLUSIONS

We have presented a complete analytical model of transient, linear flow for single-phase flow in a low-permeability, layered, and compressible reservoir on primary. Further considerations should include the effects of Buckley-Leverett displacement, as well as the effects that production and injection may have on the formation, the fluid properties, and the hydraulic diffusivity. However, the current analysis gives a good estimate of the fluid production and time-scales of interest for a heterogeneous, low-permeability, layered reservoir.

1. We have considered primary fluid recovery on the original well spacing, followed by an infill program and conversion of the infill wells to water injectors.

2. Our analysis is simplified and has many limiting assumptions. It is not meant to be a replacement for a reservoir simulation, but, being an analytical solution, it demonstrates the effects of the system parameters on the solution.
3. A single-layer analytic solution agrees well with a fully compositional numerical simulation.
4. The calculations presented here are for the South Belridge Diatomite and should give reasonable estimates of the diatomite layer productivities.
5. We give an estimate of when to drill an infill well and how long to produce from the infill well before converting it to an injector. Our analysis predicts that about 9% of OOIP can be recovered on 2-1/2-acre primary in a good portion of the South Belridge Diatomite. The infill to 1-1/4 acres, followed by a conversion of the infill well to a water injector, increases the ultimate recovery by another 3% of OOIP.
6. Hence, in the absence of a strong Buckley-Leverett banking of the oil and/or strong capillary imbibition, the effect of pressure support by water injection on the incremental oil recovery is weak. In lower quality reservoirs (layers or fields), the effect of waterflood may be small.
7. Another important result is the quantification of reservoir heterogeneity. This analysis helps identify the good layers and those layers with fast pressure responses.
8. The current analysis gives a good estimate for the pressure, production rate, and cumulative production from original wells, with infill producers drilled at some later time and then converted to water injectors. Our model can predict the onset of pressure depletion and quantify the duration of production from the infill wells before injecting water.
9. We show that producing from the infill well for a few years significantly accelerates the production from the field and can minimize the loss of production at the infill well caused by conversion to a waterflood injector.

ACKNOWLEDGEMENTS

This work was supported by two members of the U.C. Oil® Consortium, Chevron Petroleum Technology Company, and Aera Energy, LLC. Partial support was also provided by the Assistant Secretary for Fossil Energy, Office of Gas and Petroleum Technology, under contract No. DE-ACO3-76FS00098 to the Lawrence Berkeley National Laboratory of the University of California.

NOMENCLATURE

°API = oil gravity

A = twice the area of the production hydrofracture, ft^2

B = volume formation factor, RB/STB or RB/scf

c = compressibility, 1/psi

erfc= complimentary error function

GOR = gas-oil ratio, scf gas/STB oil

k = absolute permeability of the formation, millidarcies

k_{ro} = relative permeability for oil

k_{rw} = relative permeability for water

k_{rg} = relative permeability for gas

k_{row} = relative permeability for two-phase oil/water system

k_{rog} = relative permeability for two-phase oil/gas system

k_{rocw} = relative permeability to oil at connate water saturation

k_{rwro} = relative permeability to water at residual oil saturation

k_{rgro} = relative permeability to gas at residual oil saturation

L = half-spacing of original wells, ft

m = summation index

n = summation index

n_w = water relative permeability exponent

n_{ow} = oil/water relative permeability exponent

n_{og} = oil/gas relative permeability exponent

n_g = gas relative permeability exponent

P = absolute pressure in the formation, psia

p = pressure in analytical solution, psia

$\overline{p}$ = average pressure in analytical solution, psia

p_{bp} = bubblepoint pressure, psia

p_i = initial formation pressure, psia

p_{inj} = pressure in injection superposition equations, psia

p_{inject} = water injection pressure, psia

p_{net} = net (total) pressure with infill and injection, psia

p_{well} = well flowing pressure, psia

Q = cumulative amount, MB

q = flow rate, MBPD

R_s = dissolved gas-oil ratio, scf/STB

R_{sw} = dissolved gas-water ratio, scf/STB

S_{wc} = connate water saturation

S_{orw} = residual oil/water saturation

S_{org} = residual oil/gas saturation

S_{gr} = residual gas saturation

T = temperature in the formation, °F

t = time after original production begins, days

t_{inf} = time when infill well begins production, days

t_{inj} = time when water injection begins, days

WOR = water-oil ratio, STB water/STB oil

x = distance from centerline between original wells, ft

Greek Symbols

α = total fluid mobility, ft^2/day

β_m = eigenvalue

γ_g^o = gravity of gas dissolved in oil at a given pressure

γ_g = gravity of separator gas (sum of free gas and solution gas)

γ_o = oil gravity

μ = viscosity, cp

λ = mobility, md/cp

λ_n = eigenvalue

ϕ = porosity

Subscripts

f = formation

g = gas

inf = infill

inj = injection

o = oil

t = total

w = water

Superscripts

(1) = original well

(2) = infill well

net = total including infill and injection

REFERENCES

1. Schwartz, D. E.: "Characterizing the Lithology, Petrophysical Properties, and Depositional Setting of the Belridge Diatomite, South Belridge Field, Kern County, California," Studies of the Geology of the San Joaquin Basin, S. A. Graham and H. C. Olson (eds.), The Pacific Section Society

of Economic Paleontologists and Mineralogists, Los Angeles, CA (1988) 281-301.

2. Patzek, T. W.: "Surveillance of South Belridge Diatomite," paper SPE 24040 presented at the 1992 Soc. Pet. Eng. Western Regional Meeting, Bakersfield, CA, Mar. 30 - Apr. 1.

3. Nikravesh, M., A. R. Kovscek, and T. W. Patzek: "Prediction of Formation Damage During Fluid Injection into Fractured Low-Permeability Reservoirs Via Neural Network," The SPE Formation Damage Symposium, Lafayette, LA, February 14-15, 1995.

4. Nikravesh, M., A. R. Kovscek, A. S. Murer, and T. W. Patzek: "Neural Networks for Field-Wise Waterflood Management in Low-Permeability, Fractured Oil Reservoirs," paper 35721 presented at the 66th Soc. Pet. Eng. Western Regional Meeting, Anchorage, AK, May 22-24, 1996.

5. Kovscek, A. R., R. M. Johnston, and T. W. Patzek: "Interpretation of Hydrofracture Geometry Using Temperature Transients I: Model Formulation and Verification," In Situ 9, 221-250 (Sept. 1996).

6. Kovscek, A. R., R. M. Johnston, and T. W. Patzek: "Interpretation of Hydrofracture Geometry Using Temperature Transients II: Asymmetric Hydrofractures," In Situ 9, 251-289 (Sept. 1996).

7. Carslaw, H. S., and J. C. Jeager: Conduction of Heat in Solids, 2nd Ed., Clarendon Press, Oxford (1959).

8. Ahmed, T.: Hydrocarbon Phase Behavior, Contributions in Petroleum Geology and Engineering 7, Gulf Publishing Company, Houston, TX (1989) 424.

9. Standing, M. B.: A Pressure-Volume-Temperature Correlation for Mixtures of California Oils and Gases, API Drilling and Production Practice 275 (1947).

10. Beggs, H. D., and J. R. Robinson: "Estimating the Viscosity of Crude Oil Systems," Journal of Petroleum Technology 27 (1975) 1140-1141.

11. THERM, Scientific Software-Intercomp, Inc., 1801 California, Suite 295, Denver, CO 80202-2699.

APPENDIX A: Total Hydraulic Diffusivity and PVT Properties of Oil, Gas and Water

All of the formation and fluid properties are combined into the single parameter α, the hydraulic diffusivity of the fluid-rock system. We assume that α is constant and calculated using the initial formation and fluid conditions such as pressure, temperature, saturation, etc. We define α by

$$\alpha = 0.006336\frac{\lambda_t}{\phi c_t}, \quad \text{ft}^2 / \text{day} \tag{A.1}$$

where λ_t is the total fluid mobility in the reservoir, md/cp, ϕ is the porosity, and c_t is the total volume-weighted compressibility, 1/psi, of the system consisting of rock, f, oil, o, water, w, and gas, g.

The total fluid mobility is

$$\lambda_t = \lambda_o + \lambda_w + \lambda_g, \tag{A.2}$$

or

$$\lambda_t = \lambda_o\left(1 + \lambda_w / \lambda_o + \lambda_g / \lambda_o\right), \quad \text{md / cp}. \tag{A.3}$$

This equation for the total mobility can be expressed through the surface-measured quantities: the water-oil ratio, WOR in STB water/STB oil, and the gas-oil ratio, GOR, scf gas/STB oil

$$\lambda_t = \lambda_o\left(1 + \text{WOR}\frac{B_w}{B_o} + \text{GOR}\frac{B_g}{B_o}\right), \tag{A.4}$$

where B_o is the oil volume formation factor, RB/STB, B_w is the water volume formation factor, RB/STB, and B_g is the gas volume formation factor, RB/scf.

The oil mobility is defined as

$$\lambda_o = \frac{kk_{ro}}{\mu_o} \tag{A.5}$$

We use the Stone II model given later in this Appendix to calculate the oil relative permeability.

The total system compressibility is

$$c_t = c_f + S_o c_o + S_w c_w + S_g c_g, \quad 1/\text{psi} \tag{A.6}$$

which can be calculated as

$$c_t = c_f + S_o\left(-\frac{1}{B_o}\frac{\partial B_o}{\partial P} + \frac{B_g}{B_o}\frac{\partial R_s}{\partial P}\right) + S_w\left(-\frac{1}{B_w}\frac{\partial B_w}{\partial P} + \frac{B_g}{B_w}\frac{\partial R_{sw}}{\partial P}\right) - \frac{S_g}{B_g}\frac{\partial B_g}{\partial P} \tag{A.7}$$

We now define the functions used to calculate the PVT properties of the formation and the fluids. We calculate these properties at the bubblepoint. In what follows, we use general correlations[8-10] of the fluid PVT properties. The coefficients of these correlations have not been optimized for the diatomite crude-solution gas system.

Dissolved Gas-Oil Ratio, R_s (scf/STB)[9]

$$R_s = \gamma_g\left[(P/18.2 + 1.4)\gamma_g^o\right]^{1.2048} \tag{A.8}$$

where

$$\gamma_g^o = 10^{\{0.0125(°\text{API})-0.00091\text{T}\}}$$

Live Oil Viscosity, μ_o (cp)[10]

$$\mu_o = A\mu_{od}^B \tag{A.9}$$

where

$$A = 12.859(R_s + 200)^{-0.482}, \qquad B = 1.276(R_s + 15)^{-0.090}$$

Dead Oil Viscosity, μ_{od} (cp)[10]

$$\mu_{od} = 10^x - 1 \tag{A.10}$$

where

$$x = yT^{-0.601}, \qquad y = 10^z, \qquad z = 2.1646 - 0.033580(°\,\text{API})$$

Oil Formation Volume Factor, B_o (RB/STB)[9]

$$B_o = 0.97759 + 0.000120(F)^{1.20} \tag{A.11}$$

where

$$F = R_s\left(\gamma_g / \gamma_o\right)^{0.5} + 1.25\ T, \qquad \gamma_o = 141.5 / (131.5 + ^\circ \text{API})$$

Gas Formation Volume Factor, B_g (RB/scf)[9]

$$B_g = 0.005035\ Z\ (T + 459.6) / P \qquad \text{(A.12)}$$

where

$$Z = A + (1 - A) / e^B + C p_{pr}^D$$

$$A = 1.39\left(T_{pr} - 0.92\right)^{0.5} - 0.36\ T_{pr} - 0.101$$

$$B = \left(0.62 - 0.23\ T_{pr}\right) p_{pr} + \left[\frac{0.066}{\left(T_{pr} - 0.86\right)} - 0.037\right] p_{pr}^2 + \frac{0.32}{10^{9\left(T_{pr} - 1\right)}}\ p_{pr}^6$$

$$C = \left(0.132 - 0.32\ \log_{10} T_{pr}\right)$$

$$D = 10^{\left(0.3106 - 0.49 T_{pr} + 0.1824 T_{pr}^2\right)}$$

$$T_{pr} = (T + 459.6) / T'_{pcM}$$

$$p_{pr} = P / p'_{pcM}$$

$$T'_{pcM} = T_{pcM} - \varepsilon$$

$$p'_{pcm} = \frac{p_{pcM}\left(T_{pcM} - \varepsilon\right)}{T_{pcM} + y_{\mathrm{H_2S}}\left(1 - y_{\mathrm{H_2S}}\right)\varepsilon}$$

$$\varepsilon = 120\left[\left(y_{\mathrm{CO_2}} + y_{\mathrm{H_2S}}\right)^{0.9} - \left(y_{\mathrm{CO_2}} + y_{\mathrm{H_2S}}\right)^{1.6}\right] + 15\left(y_{\mathrm{CO_2}}^{0.5} - y_{\mathrm{H_2S}}^4\right)$$

$$T_{pcM} = \left(1 - y_{\mathrm{N_2}} - y_{\mathrm{CO_2}} - y_{\mathrm{H_2S}}\right) T_{pcHC} + 227\, y_{\mathrm{N_2}} + 548\, y_{\mathrm{CO_2}} + 672\, y_{\mathrm{H_2S}}$$

$$p_{pcM} = \left(1 - y_{\mathrm{N_2}} - y_{\mathrm{CO_2}} - y_{\mathrm{H_2S}}\right) p_{pcHC} + 493\, y_{\mathrm{N_2}} + 1071\, y_{\mathrm{CO_2}} + 1306\, y_{\mathrm{H_2S}}$$

$$T_{pcHC} = 187 + 330\,\gamma_{gHC} - 71.5\,\gamma_{gHC}^2$$

$$p_{pcHC} = 706 - 51.7\,\gamma_{gHC} - 11.1\,\gamma_{gHC}^2$$

$$\gamma_{gHC} = \frac{\gamma_g - 0.967\, y_{\mathrm{N_2}} - 1.52\, y_{\mathrm{CO_2}} - 1.18\, y_{\mathrm{H_2S}}}{1 - y_{\mathrm{N_2}} - y_{\mathrm{CO_2}} - y_{\mathrm{H_2S}}}$$

$y_{\mathrm{CO_2}}$ = mole fraction of CO_2 in gas phase

$y_{\mathrm{H_2S}}$ = mole fraction of H_2S in gas phase

$y_{\mathrm{N_2}}$ = mole fraction of N_2 in gas phase

Water Formation Volume Factor, B_w (RB/STB)

$$B_w = 1 \tag{A.13}$$

Oil Compressibility, (1/psi)

$$c_o = -\frac{1}{B_o}\frac{\partial B_o}{\partial P} + \frac{B_g}{B_o}\frac{\partial R_s}{\partial P} \tag{A.14}$$

where

$$\frac{\partial B_o}{\partial P} = \left[\frac{0.000144 R_s}{0.83001P + 21.14874}\right]\left(\gamma_g / \gamma_o\right)^{0.5} F^{0.2}$$

$$\frac{\partial R_s}{\partial P} = \left[\frac{R_s}{0.83001P + 21.14874}\right]$$

Gas Compressibility, (1/psi)

$$c_g = -\frac{1}{B_g}\frac{\partial B_g}{\partial P} \tag{A.15}$$

The derivative was approximated by

$$\frac{\partial B_g}{\partial P} \approx \frac{\Delta B_g}{\Delta P} = \frac{B_g[P+10] - B_g[P]}{10} \tag{A.16}$$

Water Compressibility, c_w (1/psi)[8]

$$\begin{aligned} c_w = {} & [3.8546 - 0.000134\,P \\ & + T\left(4.77\times10^{-7}\,P - 0.01052 + \left(3.9267\times10^{-5} - 8.8\times10^{-10}\,P\right)T\right)]\times10^{-6} \end{aligned} \tag{A.17}$$

Stone II Model for Relative Permeability, k_{ro}

The Stone II model uses the results of two-phase relative permeability expressions in an equation for the three-phase oil relative permeability. The two-phase expressions are power functions given as

$$k_{rw} = k_{rwro}\left[\frac{S_w - S_{wc}}{1 - S_{orw} - S_{wc}}\right]^{n_w} \tag{A.18}$$

$$k_{row} = k_{rocw}\left[\frac{1 - S_w - S_{orw}}{1 - S_{orw} - S_{wc}}\right]^{n_{ow}} \tag{A.19}$$

$$k_{rog} = k_{rocw}\left[\frac{1 - S_{wc} - S_{org} - S_g}{1 - S_{wc} - S_{org}}\right]^{n_{og}} \tag{A.20}$$

$$k_{rg} = k_{rgro}\left[\frac{S_g - S_{gr}}{1 - S_{wc} - S_{org} - S_{gr}}\right]^{n_g} \tag{A.21}$$

The final expression for the oil relative permeability is

$$k_{ro} = k_{rocw}\left[(\frac{k_{row}}{k_{rocw}} + k_{rw})(\frac{k_{rog}}{k_{rocw}} + k_{rg}) - k_{rw} - k_{rg}\right] \tag{A.22}$$

FIG. 1. Cumulative oil production in each layer.
No infill or injection.

FIG. 2. Percent oil recovery in the various layers
No infill or injection.

FIG. 3. Percent oil recovery or water injection versus the square root of time, $days^{1/2}$. Infill at 5 years and injection at 6 years.

FIG. 4. Percent oil recovery or water injection versus the square root of time, $days^{1/2}$. Infill at 10 years and injection at 11 years.

FIG. 5A. Pressure in layer G, psia, versus the position from infill well, feet.
Infill at 10 years and injection at 11 years.

FIG. 5B. Pressure in layer I, psia, versus the position from infill well, feet.
Infill at 10 years and injection at 11 years.

FIG. 5c. Pressure in layer K, psia, versus the position from infill well, feet.
Infill at 10 years and injection at 11 years.

FIG. 5D. Pressure in layer M, psia, versus the position from infill well, feet.
Infill at 10 years and injection at 11 years.

FIG. 6. Comparison of THERM simulation and analytical solution.
Percent oil recovery on primary for 50 years.

FIG. 7. Comparison of THERM simulation and analytical solution.
Average layer pressure on primary for 50 years.

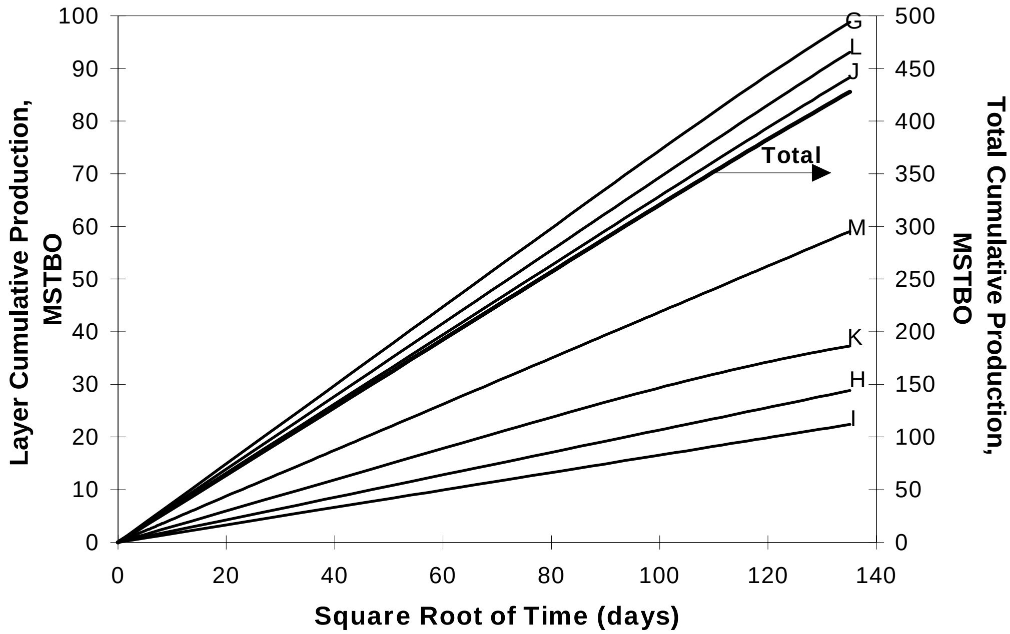

Layer Cumulative Production, MSTBO
Total Cumulative Production, MSTBO
Square Root of Time (days)
Total
G
L
J
M
K
H
I
0
10
20
30
40
50
60
70
80
90
100
0
50
100
150
200
250
300
350
400
450
500
0
20
40
60
80
100
120
140

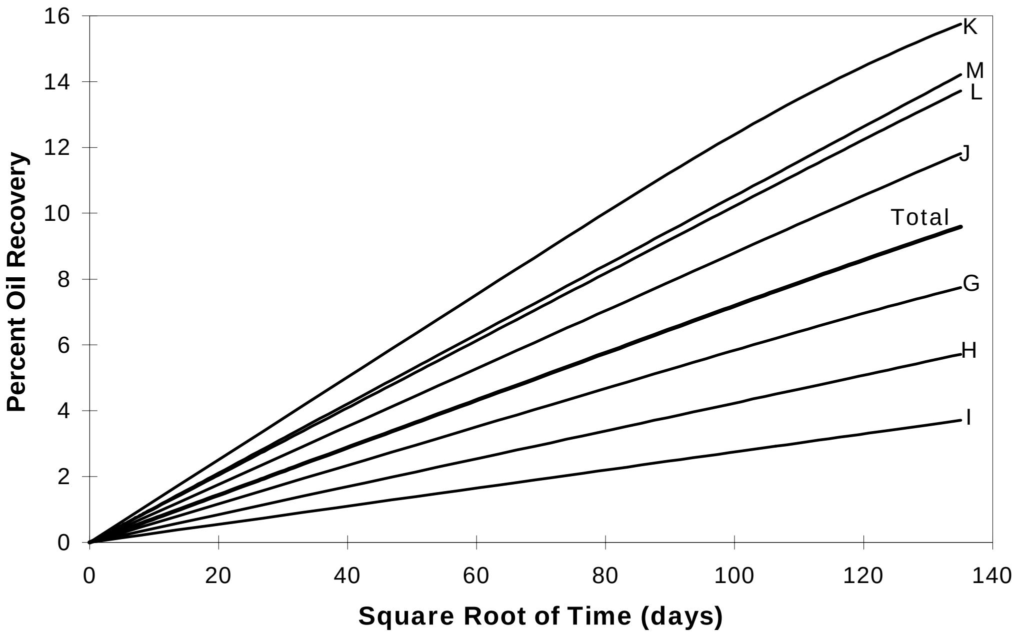

Percent Oil Recovery
Square Root of Time (days)
0
2
4
6
8
10
12
14
16
0
20
40
60
80
100
120
140
K
M
L
J
Total
G
H
I

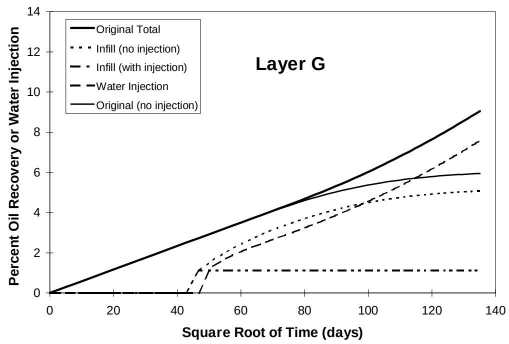
Layer G
Original Total
Infill (no injection)
Infill (with injection)
Water Injection
Original (no injection)
Percent Oil Recovery or Water Injection
Square Root of Time (days)

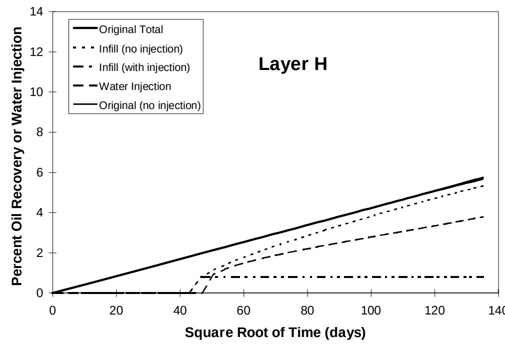
Layer H
Original Total
Infill (no injection)
Infill (with injection)
Water Injection
Original (no injection)
Percent Oil Recovery or Water Injection
Square Root of Time (days)

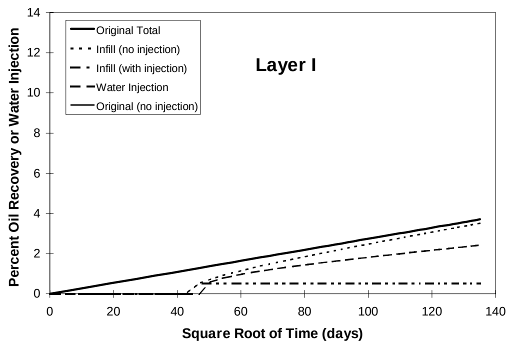
Layer I
Original Total
Infill (no injection)
Infill (with injection)
Water Injection
Original (no injection)
Percent Oil Recovery or Water Injection
Square Root of Time (days)

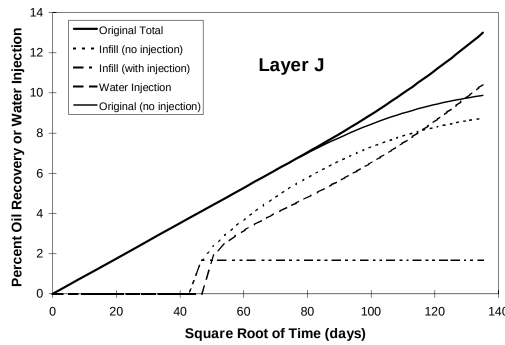
Layer J
Original Total
Infill (no injection)
Infill (with injection)
Water Injection
Original (no injection)
Percent Oil Recovery or Water Injection
Square Root of Time (days)

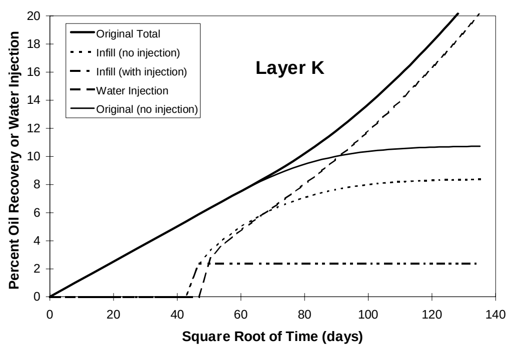
Layer K
Original Total
Infill (no injection)
Infill (with injection)
Water Injection
Original (no injection)
Percent Oil Recovery or Water Injection
Square Root of Time (days)

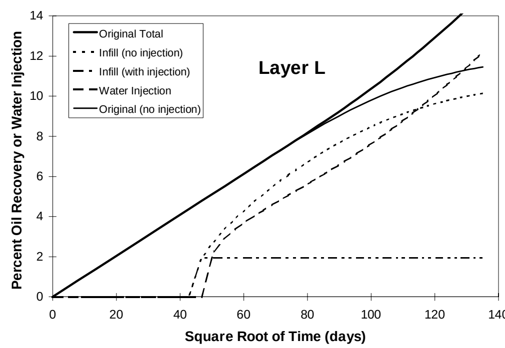
Layer L
Original Total
Infill (no injection)
Infill (with injection)
Water Injection
Original (no injection)
Percent Oil Recovery or Water Injection
Square Root of Time (days)

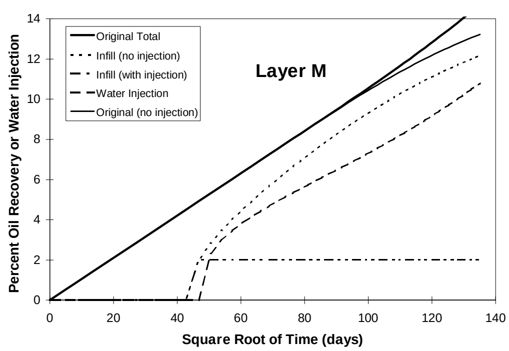
Layer M
Original Total
Infill (no injection)
Infill (with injection)
Water Injection
Original (no injection)
Percent Oil Recovery or Water Injection
Square Root of Time (days)

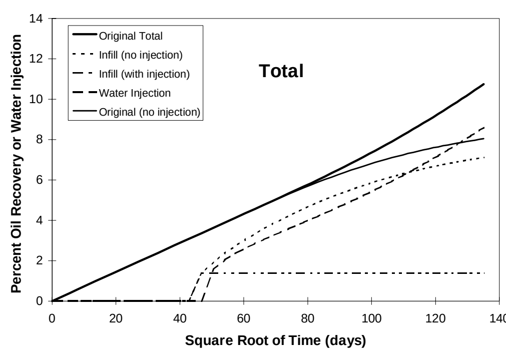
Total
Original Total
Infill (no injection)
Infill (with injection)
Water Injection
Original (no injection)
Percent Oil Recovery or Water Injection
Square Root of Time (days)

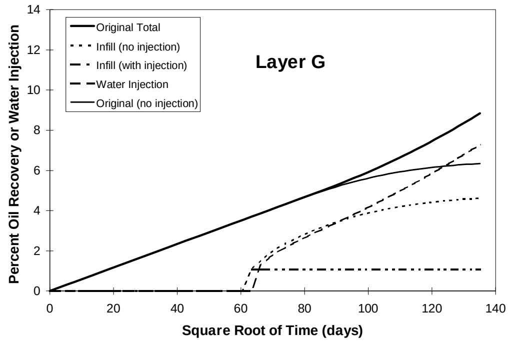
Layer G
Original Total
Infill (no injection)
Infill (with injection)
Water Injection
Original (no injection)
Percent Oil Recovery or Water Injection
Square Root of Time (days)

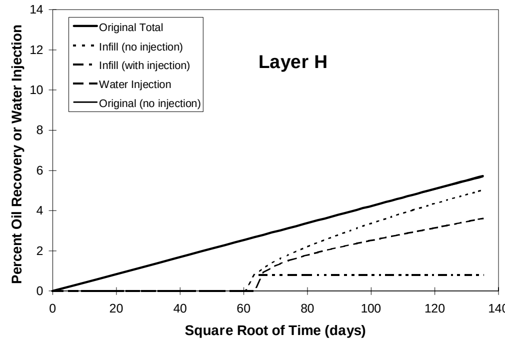
Layer H
Original Total
Infill (no injection)
Infill (with injection)
Water Injection
Original (no injection)
Percent Oil Recovery or Water Injection
Square Root of Time (days)

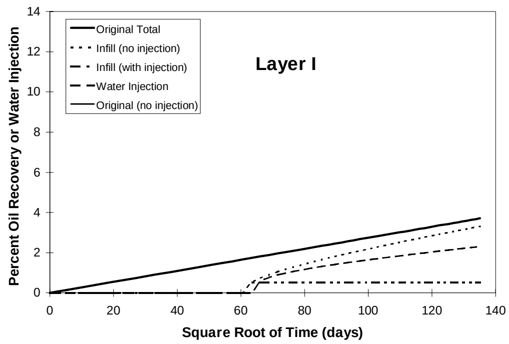
Layer I
Original Total
Infill (no injection)
Infill (with injection)
Water Injection
Original (no injection)
Percent Oil Recovery or Water Injection
Square Root of Time (days)

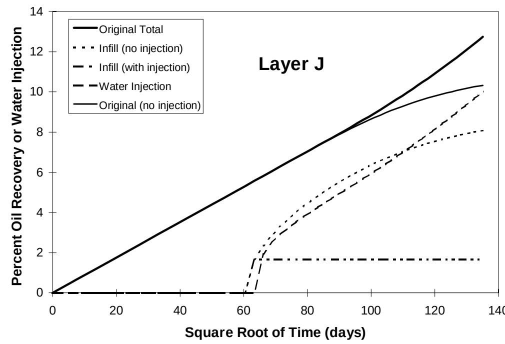
Layer J
Original Total
Infill (no injection)
Infill (with injection)
Water Injection
Original (no injection)
Percent Oil Recovery or Water Injection
Square Root of Time (days)

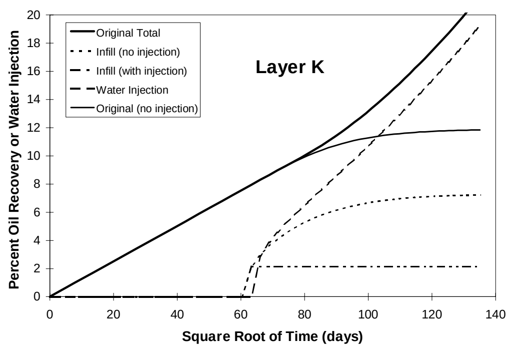
Layer K
Original Total
Infill (no injection)
Infill (with injection)
Water Injection
Original (no injection)
Percent Oil Recovery or Water Injection
Square Root of Time (days)

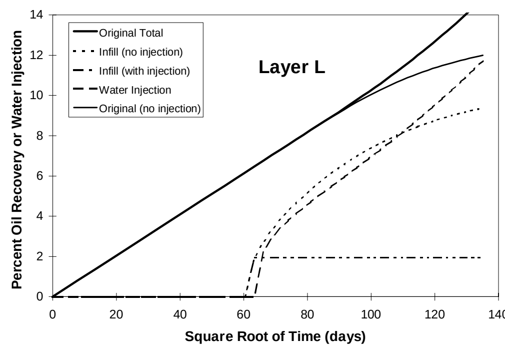
Layer L
Original Total
Infill (no injection)
Infill (with injection)
Water Injection
Original (no injection)
Percent Oil Recovery or Water Injection
Square Root of Time (days)

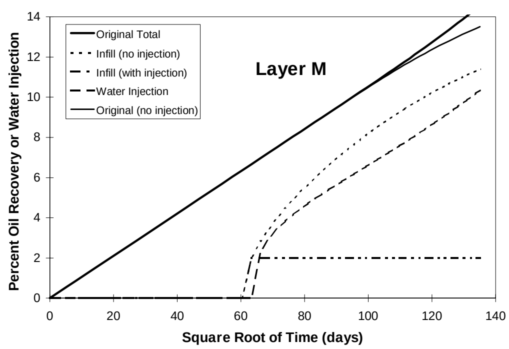
Layer M
Original Total
Infill (no injection)
Infill (with injection)
Water Injection
Original (no injection)
Percent Oil Recovery or Water Injection
Square Root of Time (days)

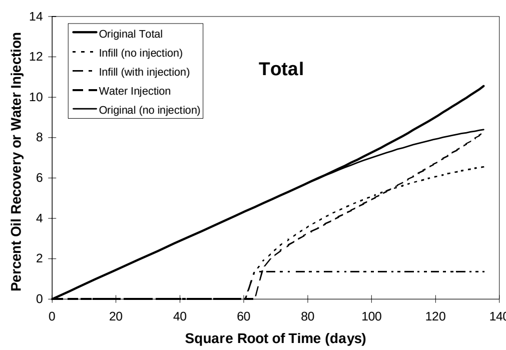
Total
Original Total
Infill (no injection)
Infill (with injection)
Water Injection
Original (no injection)
Percent Oil Recovery or Water Injection
Square Root of Time (days)

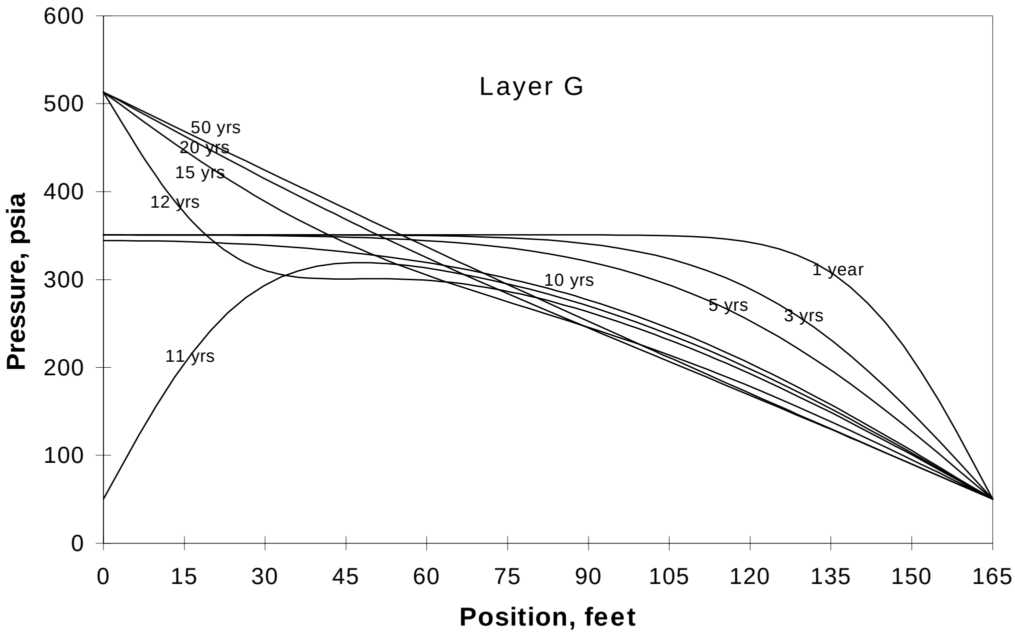

Layer G
Pressure, psia
Position, feet
600
500
400
300
200
100
0
0
15
30
45
60
75
90
105
120
135
150
165
50 yrs
20 yrs
15 yrs
12 yrs
11 yrs
10 yrs
5 yrs
3 yrs
1 year

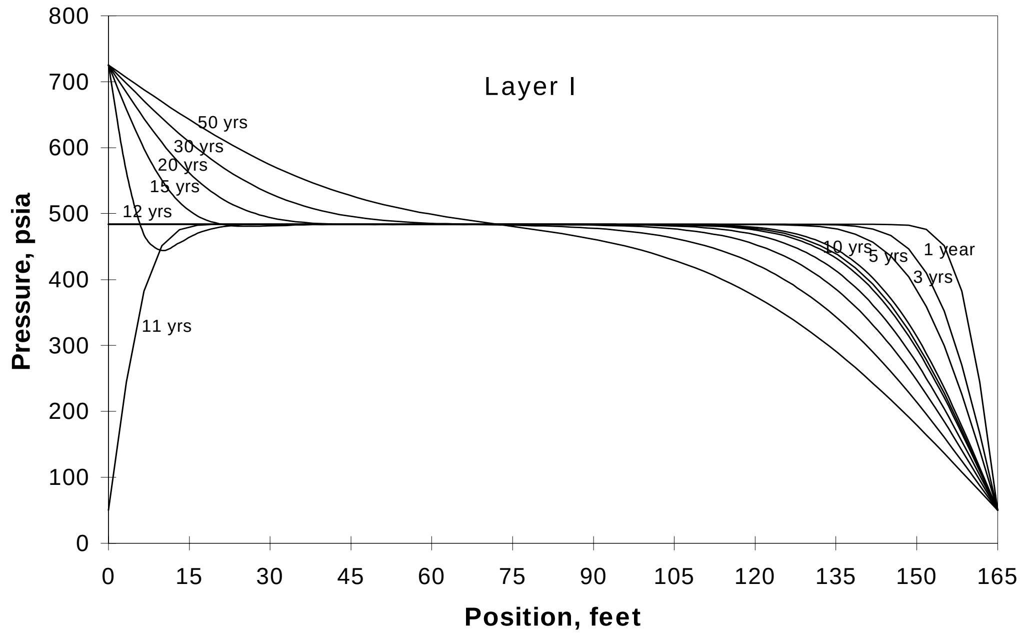
Layer I
Pressure, psia
Position, feet
800
700
600
500
400
300
200
100
0
0
15
30
45
60
75
90
105
120
135
150
165
50 yrs
30 yrs
20 yrs
15 yrs
12 yrs
11 yrs
10 yrs
5 yrs
3 yrs
1 year

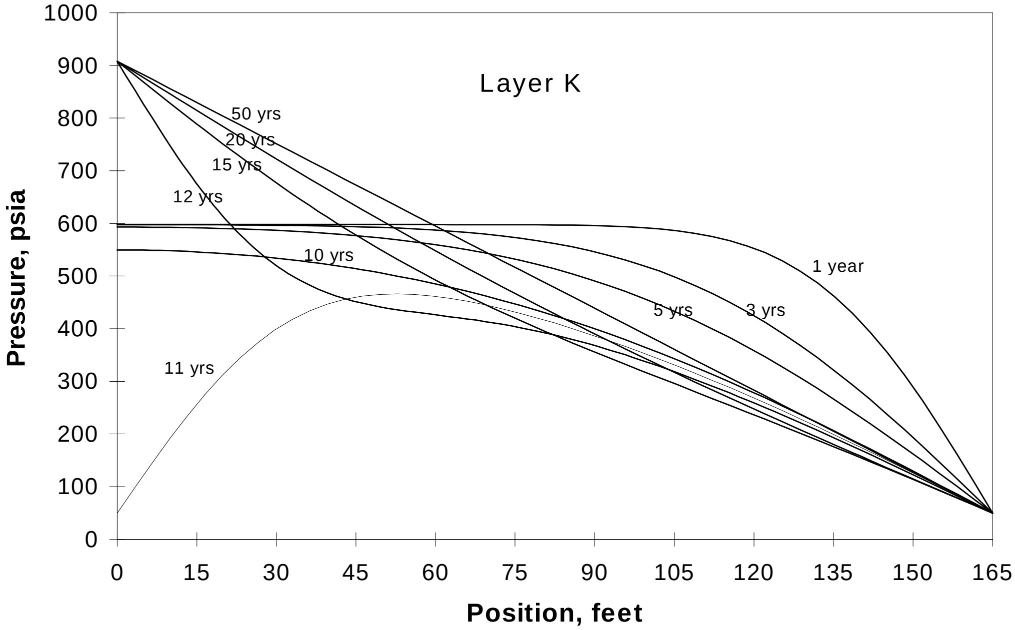

Layer K
Pressure, psia
Position, feet
1000
900
800
700
600
500
400
300
200
100
0
0
15
30
45
60
75
90
105
120
135
150
165
50 yrs
20 yrs
15 yrs
12 yrs
10 yrs
11 yrs
5 yrs
3 yrs
1 year

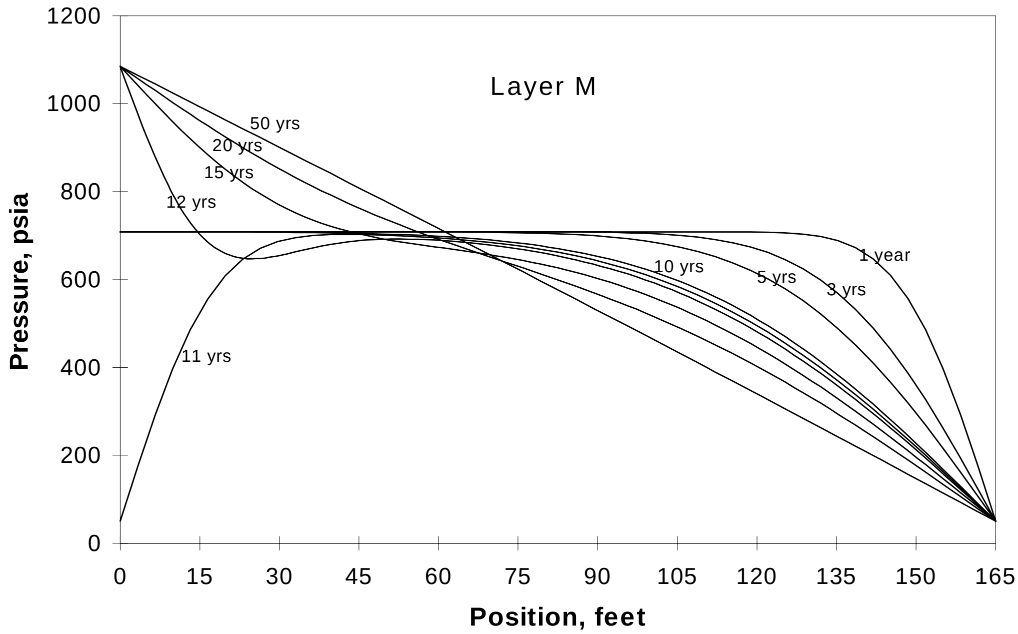
Layer M
Pressure, psia
Position, feet
1200
1000
800
600
400
200
0
0
15
30
45
60
75
90
105
120
135
150
165
50 yrs
20 yrs
15 yrs
12 yrs
11 yrs
10 yrs
5 yrs
3 yrs
1 year

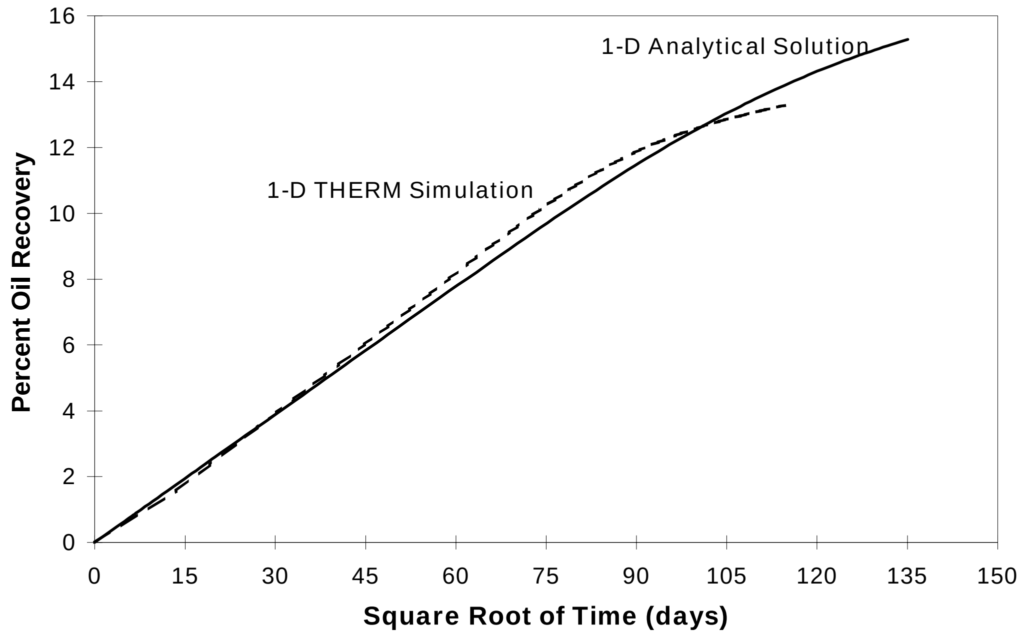
1-D Analytical Solution
1-D THERM Simulation
Percent Oil Recovery
Square Root of Time (days)
0
2
4
6
8
10
12
14
16
0
15
30
45
60
75
90
105
120
135
150

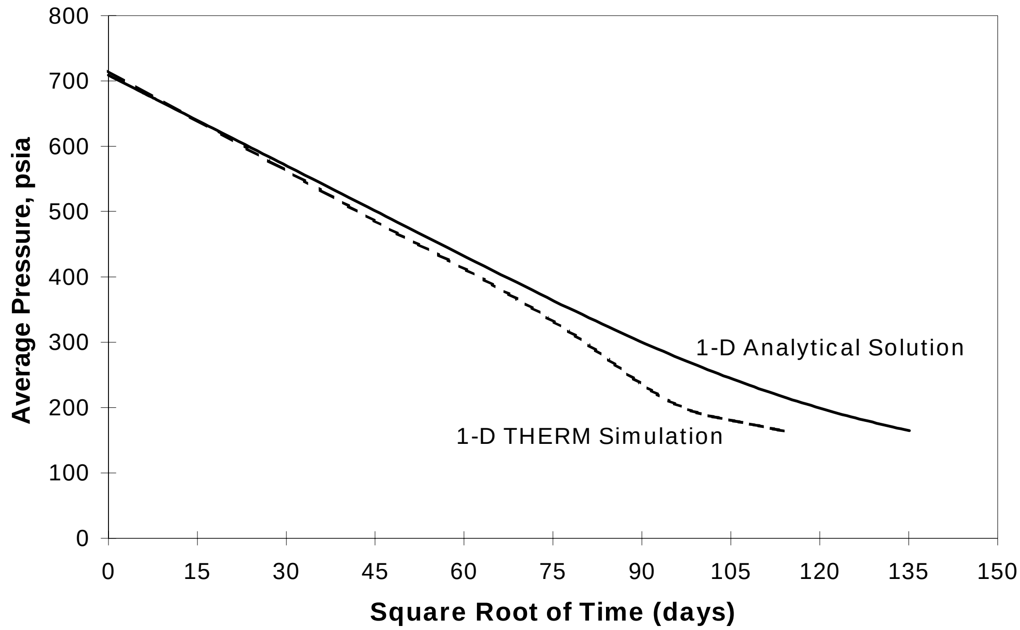

Average Pressure, psia
800
700
600
500
400
300
200
100
0
0
15
30
45
60
75
90
105
120
135
150
Square Root of Time (days)
1-D Analytical Solution
1-D THERM Simulation